Available online at www.sciencedirect.com
SCIENCE DIRECT®
PERGAMON
International Journal of Heat and Mass Transfer 46 (2003) 1599–1605
International Journal of HEAT and MASS TRANSFER
www.elsevier.com/locate/ijhmt

Magnetic field effects upon heat transfer for laminar flow of electrically conducting liquid over a melting slab

R.V. Seeniraj *, N.P. Kannan [1]

Department of Mechanical Engineering, College of Engineering, Anna University, Chennai 600 025, India

Received 2 November 2001; received in revised form 23 September 2002

Abstract

A mathematical model is presented to study the role of an applied magnetic field on heat transfer during melting of a semi-infinite slab swept by a laminar flow of an electrically conducting liquid. The integral forms of the governing equations were solved by taking into account the sensitivity of the velocity profile to the magnetic field. Numerical results were obtained for a specified set of characteristic dimensionless numbers, i.e. Reynolds number, Prandtl number, Stefan numbers and magnetic parameter and their influence on heat transfer and melt generation is reported.

1. Introduction

The use of magnetic field that influences melting/freezing process in electrically conducting fluid flows has important engineering applications. Some examples include the magnetic control of convection currents in semiconductor material processing [1], magnetic control of molten cast metals [2,3] and liquid metal flow situations [4]. The present paper is concerned with such a related problem, viz., the study of the effect of magnetic field on the laminar, incompressible, weakly electrically conducting fluid flow over a slab that melts at steady rate wherein both the flowing liquid and the melting solid slab are of the same material. A few referred works of the extensive literature available on the magnetohydrodynamic (MHD) and melting heat transfer problems are stated below.

Earlier studies on MHD problems pertain to the magnetic field effects on the fluid dynamics and heat transfer in various geometries. These analytical investigations employed both similarity techniques [5–7] and approximate integral method [8,9]. Similarly, the problem of melting heat transfer over a flat plate has been successfully treated by both similarity [10] and integral [11] methods in the absence of magnetic field. The present study, by means of an integral analysis, deals with the coupled problem of hydromagnetic flow and melting.

2. Mathematical analysis

2.1. The physical model

Fig. 1 shows the physical model. An electrically conducting liquid at temperature $\overline{T}_\infty$ and under impressed constant non-zero pressure gradient flows with a constant free-stream velocity $\overline{U}_\infty$ over a semi-infinite slab. This slab initially at $\overline{T}_o$ is subjected to a step-change in temperature to that of the free-stream and consequently transient state prevails in the solid. At steady state flow conditions, the slab surface reaches its melting temperature $\overline{T}_f$ and melts at a steady rate $\overline{V}_F$ locally and the melt is swept away continuously by the flowing warm liquid of the same material. A uniform, steady magnetic field of strength B_o is imposed perpendicular to the direction of the flow. The direction of various velocities, the flow near the boundary between the solid and the liquid and the co-ordinate system fixed to the interface are shown in Fig. 1. The phase change occurs at steady-state conditions so that the co-ordinate system is fixed to the melt interface of the solid [10–12].

* Corresponding author. Tel.: +91-44-235-1723-3265; fax: +91-44-235-0397.
E-mail address: seenirajr@hotmail.com (R.V. Seeniraj).
[1] Present address: School of Mechanical Engineering, Purdue University, West Lafayette, IN 47907, USA.

0017-9310/03/$ - see front matter
PII: S0017-9310(02)00436-2

Nomenclature

a	coefficients in the temperature profile
b	coefficients in the velocity profile
$\mathbf{B}$	magnetic induction in the liquid
B_o	applied magnetic field strength in the $\bar{y}$-direction
C_p	specific heat
D	melting parameter
$\mathbf{E}$	electric field intensity in the liquid
Ec	Eckert number
$\mathbf{e_x}$, $\mathbf{e_y}$	unit vectors in the $\bar{x}$ and $\bar{y}$-directions respectively
h	local heat transfer coefficient
$\mathbf{J}$	electric current density in the liquid
k	thermal conductivity
L	characteristic length scale in the $\bar{x}$-direction
$\overline{M}$	latent heat of melting
M	magnetic influence parameter
$\dot{m}$	rate of melt generation per unit area
Nu	Nusselt number
Pe	Peclet number
Pr	Prandtl number
Re	Reynolds number
Ste	Stefan number
$\overline{T}, T$	local and normalized temperature
$\overline{U}, U$	local and normalized axial components of velocity
$\overline{V}, V$	local and normalized normal components of velocity
$\mathbf{V}$	velocity vector in the liquid flow field
$\bar{x}, x$	local and normalized axial co-ordinate
$\bar{y}, y$	local and normalized normal co-ordinate

Greek symbols

α	thermal diffusivity
$\bar{\delta}, \delta$	local and normalized boundary layer thickness
Δ	ratio of thermal to momentum boundary layer thickness
η	normalized y—co-ordinate with respect to δ_t
κ	ratio of liquid to solid thermal conductivity
λ	ratio of maximum temperature difference in the liquid to that in the solid
ν	kinematic viscosity
ω	normalized y—co-ordinate with respect to δ_m
ξ	normalized velocity at the solid-liquid interface
ρ	mass density
σ	electrical conductivity

Subscripts

f, F	liquid phase, melt surface
o	conditions in the solid at large distance away from the solid-liquid interface ($\bar{y} \to -\infty$)
∞	free stream conditions
m	momentum boundary layer
s	solid phase
t	thermal boundary layer

Superscript

$\bar{}$	dimensional quantity

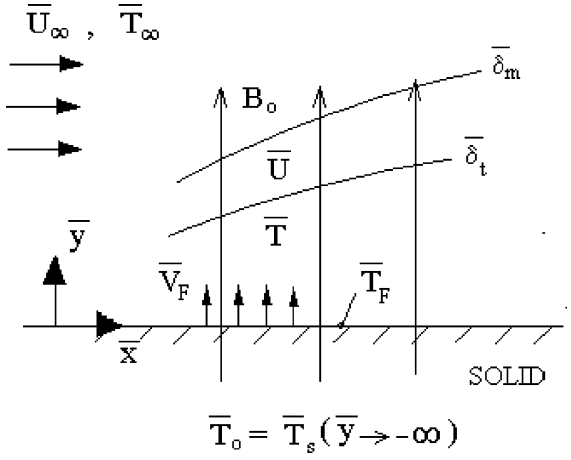

Fig. 1. Schematic diagram.

With a two-dimensional flow in the $\bar{x}$–$\bar{y}$ plane ($\mathbf{V} = \overline{U}\mathbf{e_x} + \overline{V}\mathbf{e_y}$), the application of magnetic field in the $\bar{y}$-direction ($\mathbf{B} = B_o\mathbf{e_y}$) will result in an induced current in the $\bar{z}$-direction and according to the Ohm's law, it is given by $\mathbf{J} = \sigma\,(\mathbf{E} + \mathbf{V} \times \mathbf{B})$, which in the absence of imposed electric field ($\mathbf{E} = 0$) reduces to $\sigma\overline{U}B_o$. This induced current provides a two-way coupling between the fluid flow field and the force due to magnetic induction. The resulting retarding force is referred to as Lorentz or body force per unit volume and is given by $\mathbf{J} \times \mathbf{B}$, which becomes $\sigma\overline{U}B_o^2$ and acts opposite to the positive $\bar{x}$-direction.

It should be noted that, throughout the paper, the 'bar' over the symbols indicates dimensional quantities and upon transformation into corresponding non-dimensional quantities using suitable scaling factors, they are expressed without the bar.

2.2. Basic assumptions

The following assumptions are made in this study:

(a) The applied uniform magnetic field of constant strength is considered to be fixed relative to the slab

and to act normal to the oncoming weakly conducting liquid.

(b) Both the induced magnetic field and displacement field are negligible.

(c) Though applied magnetic field will alter the velocities in the boundary layer, the flow is stable and laminar.

(d) All thermo-physical properties of the liquid/solid are constant.

(e) In this steady, two-dimensional, stable, incompressible flow, the influence of the melt addition on the magnetic field is negligible.

2.3. Mathematical formulation

The assumptions stated above permit the formulation of the problem in a manageable form. For brevity, only the system of non-dimensional form of the equations is presented. The transformation relations between the dimensional and non-dimensional quantities are:

$$x=\frac{\bar{x}}{L},\quad y=\frac{\bar{y}}{L},\quad \delta_m=\frac{\bar{\delta}_m}{L},\quad \delta_t=\frac{\bar{\delta}_t}{L},\quad \omega=\frac{y}{\delta_m},$$

$$\eta=\frac{y}{\delta_t},\quad \Delta=\frac{\delta_t}{\delta_m},\quad U=\frac{\overline{U}}{\overline{U}_\infty},\quad V=\frac{\overline{V}}{\overline{V}_F},\quad \xi=\frac{\overline{V}_F}{\overline{U}_\infty},$$

$$T=\frac{\overline{T}-\overline{T}_f}{\overline{T}_\infty-\overline{T}_f},\quad T_s=\frac{\overline{T}_s-\overline{T}_o}{\overline{T}_f-\overline{T}_o},\quad Pr=\frac{\nu_f}{\alpha_f},\quad Re_{\bar{x}}=\frac{\overline{U}_\infty\bar{x}}{\nu_f},$$

$$Re=\frac{\overline{U}_\infty L}{\nu_f},\quad Pe=RePr,\quad Nu_{\bar{x}}=\frac{h\bar{x}}{k_f},\quad M=\frac{\sigma_f B_o^2 L}{\rho_f\overline{U}_\infty},$$

$$Ec=\frac{\overline{U}_\infty^2}{C_{pf}(\overline{T}_\infty-\overline{T}_f)},\quad Ste_f=\frac{C_{pf}(\overline{T}_\infty-\overline{T}_f)}{\overline{M}},$$

$$Ste_s=\frac{C_{ps}(\overline{T}_f-\overline{T}_o)}{\overline{M}},\quad D=\frac{Ste_f}{1+Ste_s},\quad \kappa=\frac{k_f}{k_s},$$

$$\lambda=\frac{(\overline{T}_\infty-\overline{T}_f)}{(\overline{T}_f-\overline{T}_o)}$$

The continuity, momentum and energy equations in the liquid region ($0<y\leqslant\infty$) are:

$$\frac{\partial U}{\partial x}+\frac{\partial(V\xi)}{\partial y}=0 \tag{1}$$

$$U\frac{\partial U}{\partial x}+V\xi\frac{\partial U}{\partial y}=\frac{1}{Re}\frac{\partial^2 U}{\partial y^2}+M(1-U) \tag{2}$$

$$U\frac{\partial T}{\partial x}+V\xi\frac{\partial T}{\partial y}=\frac{1}{Pe}\frac{\partial^2 U}{\partial y^2}+MEcU^2 \tag{3}$$

Subject to

$$U(y=0)=0,\quad V(y=0)=1,\quad T(y=0)=0$$

$$U(y\to\infty)=1,\quad T(y\to\infty)=1 \tag{4}$$

In the momentum equation, the second term on the right-hand side (RHS) includes both the Lorentz force within the boundary layer and the effect of free-stream compensating pressure gradient in terms of the free-stream Lorentz force. Consideration of the inviscid flow momentum equation establishes the relationship between the pressure gradient and the free-stream Lorentz force [13]. The second term on the RHS of the energy equation represents the Joulean heat generation due to the induced current in the presence of magnetic field.

Assuming negligible axial conduction, the heat conduction equation in the solid region ($-\infty<y\leqslant 0$) of the melting slab may be written as

$$\frac{d^2T_s}{dy^2}-\kappa\lambda\frac{Ste_s}{Ste_f}Pe\xi\frac{dT_s}{dy}=0 \tag{5}$$

Subject to

$$T_s(y=0)=1,\quad T_s(y\to-\infty)=0 \tag{6}$$

In the above equation, the surface of the melting slab is considered to be moving at the steady-state velocity $\overline{V}_s$ [11,12] as a result of melting at the solid–liquid interface, wherein the rate at which the mass of the liquid introduced into the main stream, $\dot{m}$ is equal to the rate at which the amount of solid lost, i.e., $\rho_f\overline{V}_F(x)=\rho_s\overline{V}_s(x)$.

The energy balance at the solid–liquid interface states that the total heat transferred from the warm flowing liquid is equal to that conducted to the interior of the solid plus the latent heat supplied at the interface:

$$k_f\frac{\partial\overline{T}}{\partial\bar{y}}(\bar{y}=0^+)=\overline{M}\dot{m}L+k_s\frac{\partial\overline{T}_s}{\partial\bar{y}}(\bar{y}=0^-) \tag{7}$$

This in non-dimensional form may be written as

$$\frac{\partial T}{\partial y}(y=0^+)=\frac{Pe\xi}{Ste_f}+\frac{1}{\kappa\lambda}\frac{\partial T_s}{\partial y}(y=0^-) \tag{7a}$$

Now, Eq. (5) together with Eq. (6) may be readily integrated to yield the temperature distribution within the solid as

$$T_s=\exp\left(\kappa\lambda\frac{Ste_s}{Ste_f}Pe\xi y\right),\quad -\infty<y\leqslant 0 \tag{8}$$

This closed-form expression for the temperature distribution within the solid involves an unknown quantity, viz., the dimensionless interfacial velocity, $\xi(x)$, which will be obtained from the analysis of the liquid phase. Using the above equation in Eq. (7a) reduces the interface condition to

$$\frac{\partial T}{\partial y}(y=0)=Pe\xi\frac{(1+Ste_s)}{Ste_f}=\frac{Pe\xi}{D} \tag{9}$$

Eqs. (1)–(4) and (9) complete the mathematical formulation of the physical model.

2.4. Integral analysis approach

As exact solution to the above system is not readily possible, following the well-known approach of Karman and Pohlhausen, Eqs. (1)–(3) are integrated over the respective boundary layers and the resulting integral forms of the equations are:

$$[V(x,\delta_m)-1]\xi = -\int_0^{\delta_m} \frac{\partial U}{\partial x}\,dy \tag{10}$$

$$\frac{d}{dx}\left[\int_0^{\delta_m} U(1-U)dy\right] - \xi = \frac{1}{Re}\frac{\partial U}{\partial y}(y=0) - M\int_0^{\delta_m}(1-U)\,dy \tag{11}$$

$$\frac{d}{dx}\left[\int_0^{\delta_t} U(1-T)dy\right] - \xi = \frac{1}{Pe}\frac{\partial T}{\partial y}(y=0) - MEc\int_0^{\delta_t} U^2\,dy \tag{12}$$

The above integro-differential equations are to be solved by assuming suitable velocity and temperature profiles. Since the ponderomotive forces are present within the boundary layer, the chosen velocity has to be sensitive to changes in these forces and accordingly the boundary conditions are derived to accommodate the MHD effects. A third-order dimensionless velocity and temperature profiles are chosen:

$$U = b_0 + b_1\omega + b_2\omega^2 + b_3\omega^3 \tag{13}$$

$$T = a_0 + a_1\eta + a_2\eta^2 + a_3\eta^3 \tag{14}$$

The natural and derived boundary conditions in the velocity and thermal boundary layer respectively are:

$$U(0)=0,\quad D\frac{\partial T}{\partial \eta}(0)\frac{\partial U}{\partial \omega}(0) = Pr\Delta\frac{\partial^2 U}{\partial \omega^2}(0) + MPe\Delta\delta_m^2,$$
$$U(1)=1,\quad \frac{\partial U}{\partial \omega}(1)=0 \tag{15a–d}$$

$$T(0)=0,\quad \left[\frac{\partial T}{\partial \eta}(0)\right]^2 = \frac{1}{D}\frac{\partial^2 T}{\partial \eta^2}(0),$$
$$T(1)=1,\quad \frac{\partial T}{\partial \eta}(1)=0 \tag{16a–d}$$

The coefficients evaluated by applying the boundary conditions for U and T respectively are:

$$b_0=0,\quad b_1=\phi(6+MRe\delta_m^2),$$
$$b_2=3-2b_1,\quad b_3=b_1-2 \tag{16e–h}$$

$$a_0=0,\quad a_1=\frac{2}{D}\left[\sqrt{1+\frac{3}{2}D}-1\right],$$
$$a_2=3-a_1,\quad a_3=a_1-2 \tag{17a–d}$$

where

$$\phi=\phi(\Delta,Pr,D)=\frac{Pr\Delta}{4Pr\Delta+Da_1} \tag{18}$$

The boundary conditions shown in Eqs. (15b) and (16b) are obtained from the application of the momentum and energy equations respectively at the melting surface and the interface energy equation. Using the above profiles in the momentum and energy integral equations and neglecting the term representing the Joulean heating in the energy equation the following are obtained:

$$\frac{d}{dx}\left[\int_0^{\delta_m} U(1-U)\,dy\right] - \xi = \frac{b_1}{Re\delta_m} + \frac{Da_1}{Pe\Delta\delta_m} - M\int_0^{\delta_m}(1-U)\,dy \tag{19}$$

$$\frac{d}{dx}\left[\int_0^{\delta_t} U(1-T)\,dy\right] - \xi = \frac{(1+D)a_1}{Pe\Delta\delta_m} \tag{20}$$

For $\Delta \leqslant 1$, the momentum boundary layer thickness is larger than that of the thermal boundary layer and is valid for flows with the Prandtl number, Pr, of the fluid larger than one ($Pr \geqslant 1$). In this case, by evaluating the integrals in Eqs. (19) and (20) and after rearrangement, the final form of the momentum and energy equations respectively are:

$$\frac{d}{dx}\left[m_1\delta_m + m_2\delta_m^3 + m_3\delta_m^5\right] = \frac{1}{Re\delta_m}\left[6\phi + \frac{Da_1}{Pr\Delta}\right] + \frac{M\delta_m}{2}(3\phi-1) + \frac{M^2Re\phi\delta_m^3}{12} \tag{21}$$

where

$$m_1 = m_1(\Delta,Pr,D) = \frac{9}{70}(\phi-1) - \frac{12}{35}\phi^2,$$
$$m_2 = m_2(\Delta,Re,Pr,D,M) = \frac{MRe\phi}{35}\left(\frac{3}{4}-4\phi\right)$$
$$m_3 = m_3(\Delta,Re,Pr,D,M) = -\frac{1}{105}(MRe\phi)^2 \tag{22a–c}$$

$$\frac{d}{dx}[e_1\delta_m + e_2\delta_m^3] = \frac{(1+D)a_1}{Pe\Delta\delta_m} \tag{23}$$

where

$$e_1 = e_1(\Delta,Pr,D) = \frac{6\phi}{\Delta}Z + \left(\frac{1}{5}-\frac{a_1}{20}\right)\Delta^3 - \left(\frac{1}{28}-\frac{2a_1}{105}\right)\Delta^4,$$
$$e_2 = e_2(\Delta,Pr,D,M) = \frac{M\phi Z}{\Delta} \tag{24a, b}$$

$$Z = Z(\Delta,D) = \left(\frac{3}{20}-\frac{a_1}{30}\right)\Delta^3 - \left(\frac{2}{15}-\frac{a_1}{30}\right)\Delta^4 + \left(\frac{1}{28}-\frac{a_1}{105}\right)\Delta^5 \tag{25}$$

The term ϕ in the above equations and in the subsequent discussions corresponds to Eq. (18).

For $\Delta > 1$, the momentum boundary layer thickness is less than that of the thermal boundary layer and is valid for flows with $Pr < 1$. It may be readily seen that the resultant integrated momentum Eq. (21) and it's associated equation, Eq. (22) also holds good for this case and hence can be retained. Upon considering that the influence of the magnetic field is confined to the momentum boundary layer and noting that $\Delta > 1$, it can be seen that the flow field affects only a part of the temperature field. This calls for appropriate limits of integration of the energy equation, Eq. (20). The final form of the energy equation for this case is

$$\frac{\mathrm{d}}{\mathrm{d}x}\left[e_1\delta_\mathrm{m} + e_2\delta_\mathrm{m}^3\right] = \frac{(1+D)a_1}{Pe\Delta\delta_\mathrm{m}} \tag{26}$$

where

$$\begin{aligned} e_1 &= e_1(\Delta, Pr, D) \\ &= \left(\frac{\Delta}{2} + \frac{1}{50\Delta^2} - \frac{1}{14\Delta^3} - \frac{1}{2}\right) \\ &\quad + 6\phi\left(\frac{1}{12} - \frac{1}{20\Delta^2} + \frac{2}{105\Delta^3}\right) - \psi_1 \end{aligned}$$

$$e_2 = e_2(\Delta, Re, Pr, D, M) = MRe\phi\left(\frac{1}{12} - \psi_2\right) \tag{27a, b}$$

$$\begin{aligned} \psi_1 &= \psi_1(\Delta, Pr, D) \\ &= \left[\frac{\Delta}{12} + \frac{1}{2\Delta}\left(\frac{\phi}{5} - \frac{3}{20}\right)\right. \\ &\quad \left. + \frac{1}{\Delta^2}\left(\frac{2}{15} - \frac{\phi}{5}\right) + \frac{1}{\Delta^3}\left(\frac{2\phi}{35} - \frac{1}{28}\right)\right]a_1 \end{aligned}$$

$$\begin{aligned} \psi_2 &= \psi_2(\Delta, D) \\ &= \left[\frac{1}{30\Delta} - \frac{1}{30\Delta^2} + \frac{1}{105\Delta^3}\right]a_1 + \frac{1}{20\Delta^2} - \frac{2}{105\Delta^3} \end{aligned} \tag{28a, b}$$

For a chosen set of parameters Re, Pr, D, M that define the problem, above the non-linear ordinary differential equations, viz., Eqs. (21) and (23) or (26), are simultaneously solved numerically by the fourth-order Runge–Kutta method by integrating along the x-direction with a step size $\delta x = 10^{-3}$. In conjunction with the integration scheme, the Newton–Raphson iterative technique is used to solve the resulting non-linear equations at each discrete location, x by iterating the quantities δ_m and Δ till converging results are obtained for $\delta_\mathrm{m}(Re, Pr, D, M, x)$ and $\Delta(Re, Pr, D, M, x)$ with an accuracy of $\varepsilon = 10^{-4}$. Subsequently, the following quantities of interest may be computed:

The melt generation rate is obtained from Eq. (9) and (14) and using $Pe_{\bar{x}} = xPe$:

$$\frac{\overline{V}_\mathrm{F}}{\overline{U}_\infty}\sqrt{Pe_{\bar{x}}} = \frac{Da_1}{\Delta\delta_\mathrm{m}\sqrt{Pe}}x^{\frac{1}{2}} \tag{29}$$

The local Nusselt number obtained from the rate of heat transfer at the melting surface and using Eq. (14) is

$$Nu_{\bar{x}} = \frac{x}{\delta_\mathrm{t}}\frac{\partial T}{\partial \eta}(0) = \frac{xa_1}{\Delta\delta_\mathrm{m}} \tag{30}$$

Upon taking the ratio of the above case to the corresponding flow over a flat plate in the absence of both melting and magnetic field is

$$\frac{Nu_{\bar{x}}}{Nu_{\bar{x}o}} = \frac{3a_1}{\Delta\delta_\mathrm{m}}Re^{-0.5}Pr^{-0.33}x^{0.5} \tag{31}$$

It may be noted when the limiting case of a slug flow situation is considered, the governing equations become considerably simpler, yielding closed form solutions which, however, are not presented here due to space limitations.

3. Results and discussion

For brevity, only representative numerical results obtained will be discussed to study the trends. The present problem, in comparison with the conventional boundary layer problems, has the magnetic influence parameter, M and the melting parameters, i.e. the liquid (Ste_f) and solid (Ste_s) Stefan numbers as the additional parameters. In addition, there is a non-dimensional interfacial velocity due to melting, $\xi(x)$, which is unknown a priori to be evaluated. The range of values chosen for M to study its effect on the melting heat transfer is limited to steady and stable laminar flow region referred to as Hartmann boundary layer flow. For the limiting case of melting in the absence of magnetic field ($M = 0$), the computed results for the thickness of the velocity and thermal boundary layers, melt generation rate and heat transfer rate agree with those presented by Griffin [11]. Fig. 2 shows the influence of M on Δ and δ_m at a

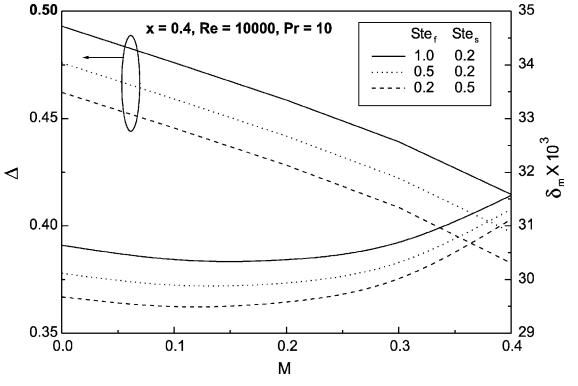

Fig. 2. Effect of M on Δ and δ_m for different Ste.

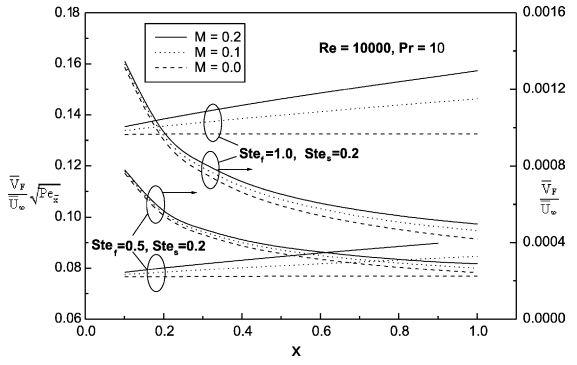

Fig. 3. Effect of M and Ste on the axial variation of the interfacial velocity and the melt generation rate.

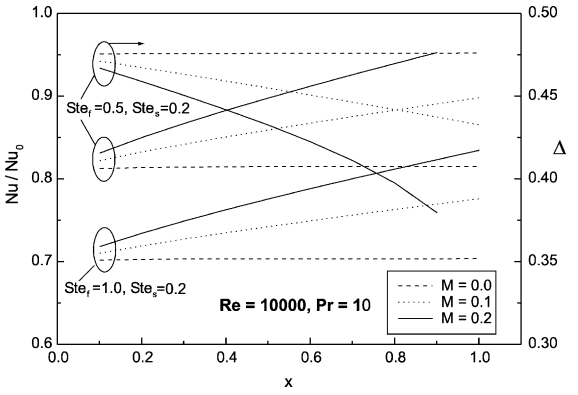

Fig. 4. Effect of M and Ste on the axial variation of Δ and the normalized Nusselt number.

specified location ($x = 0.4$) for a set of Ste_f and Ste_s. As M increases, Δ decreases in all the cases. This is due to increased Lorentz force arising from the interaction of the fluid flow and the applied magnetic field that counteracts the viscous forces. A higher value of Ste_f for a given melting temperature represents a higher value of the free stream temperature. This requires a longer path for thermal transport between the fluid stream and the melting slab resulting in increased Δ or thermal boundary layer thickness for higher Ste_f for a given M. This variation is consistent with that observed by Griffin [11] for $M = 0$.

Fig. 3 shows the axial variation of the interfacial velocity and the melt generation rate for different set of values of M, Ste_f and Ste_s. It may be seen that the interfacial velocity has a maximum value at the leading edge of the slab and decreases along the axial direction. The addition of the melt layer decreases the mean fluid temperature in the downstream of the slab reducing the interfacial velocity. At a given location, for a specified magnetic field, a higher Ste_f promotes the melting process thereby increasing the melt generation rate. The applied magnetic field though has a marginal effect in the region near to the leading edge, its influence increases away from the leading edge and has a pronounced effect at higher Ste_f. Computed results also show that the melt generation rate decreases as Ste_s increases for a given set of value of M and Ste_f as a result of increased subcooling of the solid requiring larger heat transport into the solid to bring its surface to the melting temperature. The effect of M for given Ste_f and Ste_s on the axial variation of thermal boundary layer thickness and also on the normalized Nusselt number is given in Fig. 4. It may be seen that when $M = 0$, Δ is essentially a constant along the axial direction as assumed in [11]. When the applied magnetic field is increased, the thermal boundary layer thickness decreases appreciably which becomes pronounced in the downstream of the slab. As a result, the temperature gradient at the surface of the slab increases resulting in higher heat transfer rates for higher M with greater effects in the downstream of the slab. For a constant magnetic field, an increase in Ste_f thickens the thermal boundary layer resulting in reduced heat transfer rate. These trends are consistent with the earlier finding that a combination of higher Ste_f, lower Ste_s and higher M promotes melt generation.

4. Summary

In the present work, the steady laminar boundary layer flow past a melting slab in a transverse magnetic field is studied. The boundary layer equations with attendant boundary conditions are analytically solved to study the influence of magnetic field. The imposed magnetic field has a greater influence compared with the non-magnetic case on the velocity boundary layer and promotes heat flux at the interface. Numerical results show that the ratio of the thickness of thermal to momentum boundary layer decreases with increase in the magnetic field for the chosen set of parameters. Also an increase in the local heat flux is observed in the downstream direction. Increasing the strength of the magnetic field enhances the melt generation rate in higher Prandtl number fluids.

Acknowledgements

The authors thank Dr. R. Velraj and Mr. N. Lakshmi Narasimhan in the preparation of the manuscript. The authors gratefully acknowledge the reviewers for their suggestions.

References

[1] R.W. Series, D.T.J. Hurle, The use of magnetic fields in semiconductor crystal growth, J. Cryst. Growth 113 (1991) 305–328.

[2] V. Vives, C. Perry, Effects of magnetically damped convection during the controlled solidification of metals and alloys, Int. J. Heat Mass Transfer 30 (1987) 479–496.
[3] P.A. Davidson, Magnetohydrodynamics in materials processing, Ann. Rev. Fluid Mech. 31 (1998) 273–300.
[4] T. Tagawa, H. Ozoe, Enhancement of heat transfer rate by application of a static magnetic field during natural convection of liquid Metal in a cube, ASME J. Heat Transfer 119 (1997) 265–271.
[5] V.J. Rossow, On flow of electrically conducting fluids over a flat plate in the presence of a transverse magnetic field, NACA Technical Note 3971, Washington, 1957.
[6] R.D. Cess, Magnetohydrodynamic effects upon heat transfer for laminar flow across a flat plate, ASME J. Heat Transfer 82 (1960) 87–93.
[7] M.H. Cobble, Magnetofluiddynamic flow with a pressure gradient and fluid injection, J. Eng. Math. 11 (1977) 249–256.
[8] W.C. Moffat, Analysis of MHD channel entrance flow using the momentum integral method, AIAA J. 2 (1964) 1495–1497.
[9] W.H. Heiser, W.J. Bornhorst, A modified pohlhausen velocity profile for MHD boundary layer problems, AIAA J. 4 (6) (1966) 1139–1141.
[10] M. Epstein, D.H. Cho, Melting heat transfer in steady laminar flow over a flat plate, ASME J. Heat Transfer 98 (1976) 531–533.
[11] O.M. Griffin, Heat, mass and momentum transfer during the melting of glacial ice in sea water, ASME J. Heat Transfer 95 (1973) 317–323.
[12] L. Roberts, On the melting of a semi-infinite body of ice placed in a hot stream of air, J. Fluid Mech. 4 (1958) 505–528.
[13] W.F. Hughes, F.J. Young, The Electromagnetodynamics of Fluids, John Wiley and Sons, New York, 1966.